Journal of Advances in Mechanical Engineering and Science, Vol. 4(1) 2018, pp.1-18

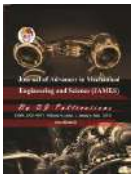

RESEARCH ARTICLE

Multi Objective Adaptive PSO for Uniform and Maximum Heat Transfer over Electronic Chips in a Channel

Abhijit Paul[1], S.K Mandal[1], *Dipak Sen[1], Prases K Mohanty[1], Asis Giri[2]
[1]Department of Mechanical Engineering,
National Institute of Technology, Yupia, Arunachal Pradesh, India.
[2]Professor, Department of Mechanical Engineering,
North Eastern Regional Institute of Science and Technology, Nirjuli, Arunachal Pradesh, India.

Received- 19 January 2018, Revised- 13 February 2018, Accepted- 20 February 2018, Published- 27 February 2018

ABSTRACT

In this paper, a numerical analysis is carried out to govern the steady laminar fluid flow and forced convection heat transfer over isothermally heated blocks affixed in lower wall of a 2-D horizontal channel. Air is considered here as a cooling fluid. A three-sided cross sectional bar is utilized as controlling element of heat flux. Parameters like different bar positions along x and y axis and bar base length are used to run the analysis with Reynolds number ($25 \leq Re \leq 400$). The variation of vortex creator position both horizontally as well as vertically influences much onto the thermal boundary layer over the blocks. The position of vortex creator closer to the upper wall as well as over the second block results in comparatively better heat transfer over the blocks within constrained parameters. Considering local Nusselt number, it is observed that the front and upper face of the blocks plays a significant role in heat transfer compared to the back faces. The Response Surface Methodology (RSM) prediction of Nusselt number corresponds well with the numerical outputs of continuity, momentum and energy equation solver. The solver used here is ANSYS 16.2. In accordance to maximize heat transfer and to maintain uniformity of heat flux, an Adaptive Particle Swarm Optimization (APSO) algorithm is deployed using MATLAB. A concept of the enhanced ϵ dominance method is introduced in multi-objective PSO algorithm to overcome the premature convergence. The Pareto optimal solutions are obtained through multi-objective PSO using the proposed algorithm.

Keywords: Uniform heat flux, Vortex creator, Heated blocks, Adaptive PSO, RSM.

1. INTRODUCTION

In order to avert thermal glitches in a number of systems of HVAC and metallurgy industry, upgrading in cooling techniques of electronic devices is essential to evade deplorable temperature increase. The design of compacted heat exchanger is a vital issue in applications of electronic cooling, automotive industry, aircraft and spacecraft. [1-4]. Various forms of vortex generators like protrusions, inclined blocks, wings, fin, ribs and winglets can be used to enhance heat transfer [5-7] in different geometries such as circular, non-circular channel under turbulent flow [8-11] as well as laminar flows [12-15]. A virtuous literature survey suggests that many studies are focused on heat transfer augmentation with the utility of different shaped control element. Unsteady flow and heat transmission in three dimensional duct installing inclined block on one of its wall is examined for Pr=.71 and Re=400-1500 [16]. An oscillating rectangular bar is used [17] to improve heat transfer of electronic equipment. The oscillating bar took active participation in vortices generation. The article adopts Gelerk in finite element method to solve the flow equations. [18] With an intension of internal flow amendment persuaded by vortex shedding, augmentation of heat transmission has been executed fruitfully

*Corresponding author. Tel.: +919485231949
Email address: dipaksen.me@gmail.com (D.Sen)
Double blind peer review under responsibility of DJ Publications
https://dx.doi.org/10.18831/james.in/2018011001

by inserting an oblique plate. In mixed convection, the output reveals that oblique plate influences a lot. [19] has presented flow loss and heat transfer augmentation installing rectangular bar in a channel for diverse periodicity lengths in a range of Reynolds number, 100-400. [20] has investigated the best possible position of a triangular bar which acts as a vortex generator in a rectangular channel for heat transfer enhancement of electronic chips. Body force and viscous dissipation are ignored. For optimization algorithm, genetic algorithm combined with Gaussian process has been used. Box and Wilson [21] first invented the Response Surface Methodology (RSM). RSM is able to build a comparatively precise prediction of input-output relationships in engineered systems and optimization of the system is designed accordingly. RSM has been vastly applied in several fields of thermal and manufacturing for the purpose of optimization [22-27]. Apart from the reduction in experimental cost, RSM is also advantageous in minimizing the variability around the target while making the performance value similar to the target value. Additionally, the optimal working condition attained from the simulation or laboratory studies can be reproduced in real applications. [28] numerically investigates the heat transfer enhancement of five electronic chips mounted on a horizontal rectangular channel in the presence of vortex generator. In this study Box Behnken design is used to find the interaction between the parameters which influence the Nusselt number.

In recent times, a number of researchers are enticed to Particle Swarm Optimization (PSO). With the intention of maximizing the anticipation as a function, for getting optimum values, this algorithm is one of the most vastly applied techniques. Through the applications of several empirics [29], PSO and GA algorithms mutually upgrades itself, which act utilizing a solution set. PSO is a route based higher level algorithm for optimization. It utilizes the concept of velocity and distance to upgrade the solution's position. Nonetheless, GA is not route based, in order to generate a new solution, it shifts the solution's building blocks, called chromosomes. [30] has developed the PSO algorithm and has been utilized by many authors [31-33], for the optimization of a cross-flow plate fin heat exchanger. The efficiency of the suggested algorithm has acquired more precise results by taking different variables. A comparison of the effectiveness of PSO and GA is done in [34] for longitudinal fin geometry, and is concluded that PSO acts more competently for geometry optimization. [35] has also presented that the PSO algorithm acted much superior than GA. [36] has used GEP and PSO to optimize forced convection heat transfer over rounded cylinder.

The above survey portrays that many studies are made for heat transfer augmentation. Also PSO has been implemented to optimize the heat transfer process in various applications. But as per our concert, PSO has never been implemented for optimization of forced convection over blocks inserted in a channel using a vortex creator using RSM predicted function. The foremost goal of present analysis is to optimize the position parameter of vortex creator along x and y axis for having a uniform as well as maximum heat transfer over the blocks. The task has been accomplished by PSO algorithm using commercial software MATLAB [37, 38], by utilizing a predicted objective function by response surface methodology. This problem belongs to constrained multi objective optimization category. In this problem, the influence of vortex creator position onto heat transfer augmentation has also been studied numerically.

2. PORTRAYAL OF ANALYZED MODEL

2.1. Nomenclature

CP:	Specific heat at constant pressure
a:	Base length of three-side bar
h:	Width and height of blocks
H:	Channel height
b:	Height of three-side bar
k:	Thermal conductivity
Re:	Reynolds number
L:	Channel length
ṁ:	Rate of flow
h0:	Coefficient of heat transfer
n:	Normal coordinate
W:	Space between blocks
p:	Pressure
Q:	Heat transfer
T:	Temperature
u,v:	Velocity components along x and y axis
ν:	Kinematic viscocity

α: Coefficient of thermal diffusivity
ρ: Density
b: Bulk
c: Cold
w: Wall

Figure A1 displays the province of computation along with boundary conditions and coordinates. It is a plane channel along with five isothermal heaters/blocks and an adiabatic three-sided cross sectional bar. With uniform velocity and temperature profile, the fluid thrusts into the duct. The fluid temperature is colder than the blocks. Along with insignificant buoyancy effects supposition, fluid thermal properties are presumed to be fixed. A fresh grid distribution is engendered for every bar location. A grid distribution for vortex creator position (x=6b, y=4.5b) is given in figure A1(b). An even grid distribution is set within the channel as viewed from the figure. It is executed using the software workbench 16.2. A finer grid is applied around the triangular bar as well as around each blocks. Real dimensions are given in table. 1.

Table 1.Exact lengths of dimensional parameters in physical model

Parameter	Dimension
A	0.25,0.5, 1,2
B	1
H	2
H	6
L	75
Y	3.5,4.5,5.5,6
X	6, 8, 11, 13
W	2

3. NUMERICAL SOLUTION

Assumptions like steady two-dimensional laminar and incompressible flow with constant fluid properties have been made to have the numerical model of fluid flow and heat transfer. Along with negligible radiation heat transferal, viscous dissipation and body forces are overlooked. Having these assumptions in mind, the governing equations are inscribed as,

$$\frac{\partial u}{\partial x}+\frac{\partial v}{\partial y}=0 \qquad (3.1)$$

$$u\frac{\partial u}{\partial x}+v\frac{\partial u}{\partial y}=-\frac{1}{\rho}\frac{\partial p}{\partial x}+v\left(\frac{\partial^2 u}{\partial x^2}+\frac{\partial^2 u}{\partial y^2}\right) \qquad (3.2)$$

$$u\frac{\partial v}{\partial x}+v\frac{\partial v}{\partial y}=-\frac{1}{\rho}\frac{\partial p}{\partial y}+v\left(\frac{\partial^2 v}{\partial x^2}+\frac{\partial^2 v}{\partial y^2}\right) \qquad (3.3)$$

$$u\frac{\partial T}{\partial x}+v\frac{\partial T}{\partial y}=\propto\left(\frac{\partial^2 T}{\partial x^2}+\frac{\partial^2 T}{\partial y^2}\right) \qquad (3.4)$$

As written in equations (3.1) to (3.4) u and v are the velocity components, p is the pressure, ν is the kinematic viscosity, ρ is the fluid density, T is the fluid temperature and α is the thermal diffusivity. The boundary conditions can be detailed as follows:

At duct inlet,

$$u=1,\ T=0 \qquad (3.5)$$

At duct outlet,

$$\frac{\partial u}{\partial x}=0,\ \frac{\partial v}{\partial x}=0,\ \frac{\partial T}{\partial x}=0 \qquad (3.6)$$

On the upper, lower wall and blocks,

$$u=v=0 \qquad (3.7)$$

On the three-sided bar

$$u=v=0,\frac{\partial T}{\partial n}=0 \qquad (3.8)$$

Involved Reynolds number is calculated as,

$$Re=\frac{uH}{v} \qquad (3.9)$$

Local heat transfer coefficient is given as,

$$-k\frac{\partial T}{\partial x}\Big|_w=h_0(T_w-T_\infty) \qquad (3.10)$$

Local Nusselt number is calculated from,

$$Nu_0=\frac{h_0 h}{k} \qquad (3.11)$$

Both local and surface averaged (mean) Nusselt numbers are computed centered on various faces of the chip as shown in figure A1(a). The bulk temperature is descripted as,

$$\mathrm{T_b}=\int_0^{\mathrm{H}}\mathrm{C_p}\rho\mathrm{u(H)HdH} \qquad (3.12)$$

The solvation of the flow and energy governing equations (3.1) to (3.4) subjected to boundary conditions (3.5 to 3.12) is

accomplished utilizing ANSYS 16.2. The method which has been exploited to solve the discretized equations is the finite volume, SIMPLE method [31].

3.1. Grid independency and validation

First of all, the numerical results of a test domain with same dimension and parameter are used by Hakan F. Oztop work [36]. The mean difference in results of present and Hakan F. Oztop's work, lies less than 4%, which is witnessed clearly in figure A2 (a-b). Hence the results of present work have been validated successfully. For grid independency test, by changing the cell number from 52k to 25k, total 5 sets of cell number have been considered with some fixed parameters. The difference % in result of Nusselt number of each block for every changed set of cell numbers lies from -0.4% to 0.4% as depicted in figure A2(c). Considering time consuming fact, least cell number 25k has been adopted to run further analysis. Thus the results of present work are grid independent, and have been proved efficaciously.

4. PARTICLE SWARM OPTIMIZATION

Along with a population of haphazard solutions, PSO is initialized and then through creating new locations [39], it upgrades its solution. Schooling of fish and bird's flocking kind of social activities motivates this algorithm [40]. Besides the necessities like less CPU memory and speed, PSO can be implemented very easily. All the particles defined as solution members hovers across the space of problem pursuing the finest performed particle as well as stalking their finest locations. With each iteration, every particle in the swarm has to upgrade itself in accordance to its velocity and position. PSO algorithm can easily achieve a local optimum [41] value; at the same time, it can also converge to a better solution very rapidly. At the time of best particle's activity, once the best particle is recognized, all other particles moves towards the best particle. Furthermore, there remains little strictures to be amend. PSO algorithm is utilized in numerous computer science and engineering applications [42-48]. Every particle in PSO is used to keep the best location, attained hitherto. Every particle upgrades their velocity from the preceding velocity utilizing the equation (4.1), while their location is attuned, it results in equation (4.2).

$$V_i(t+1) = W(t)V_i(t) + c_1 r_1(t)(pbest_i(t) - X_i(t) + c_2 r_2(t)gbest(t) - X_i(t) \quad (4.1)$$

$$X_i(t+1) = X_i(t) + V_i(t+1) \quad (4.2)$$

where $X_i(t)$: The position of the particle i at iteration t

$V_i(t)$: The velocity of the particle i at iteration t

$pbest_i(t)$: The personal best position of the particle i at iteration t

$gbest_i(t)$: The global best position among all the particles.

c_1c_2: The cognitive and social parameters which are used to maintain a balance between exploration and exploitation.

r_1r_2: The random numbers used for providing stochastic characteristics for the particle velocities.

W: Inertia weight control parameter which is required to control the previous velocity of the particles for the current velocity of each particle.

4.1. Proposed multi-objective adaptive method

In classical PSO, it is observed that the control parameter W regulates the exploratory search to an exploitation search ability of the swarm. The recommended starting value of inertia weight is large in order to enhance the global search in the search place and it keeps on decreasing gradually to get more refined solution in the local search space. In general, the inertia weight can be adaptively set according to the following equation (4.3),

$$W(t) = \frac{(max\_iter - iter)(W_{max} - W_{min})}{max\_iter} \quad (4.3)$$

where W_{max} and W_{min} are the initial and final inertial weights and max_iter is the maximum number of iterations and iter is the present iteration number. Here the inertia weight is adaptively changing with respect to the iteration number. So the proposed multi objective adaptive PSO can be effectively locate the global optimum in the search space.

The steps involved in adaptive MPSO are,

Begin
Step-1
For i=1 to N (N is the swarm size)

I. Initialize the particles position randomly.
II. Initialize $V_i(t)=0$ (V is the velocity of the particle)
III. Calculate the fitness of each particle
IV. Compare the personal best ($pbest_i$) for each particle over all previous best (X_i)
V. Find out the personal best (pbest) and global best (gbest)

End

Step-2

Non-dominated solution is constructed (initialized), which is stored in the archive (A_t).

Step-3

The global bests for each particle in the swarm are randomly selected from the archive (A_t).

Step-4

I. For iter=1 to max
II. The velocity and position of each particle i in the swarm is updated according to equation. (4.1) and (4.2). The inertia weight is updated using equation (4.3).
III. Mutation with self-adapting probability.
IV. Evaluate the fitness of each particle in swarm.
V. Each particle in swarm has a new position, if the current position is dominated by its present best position (pbest), then keep its personal best location ($pbest_i$), then the previous position is kept, otherwise the current position is treated as the personal best position, if they are mutually non-dominated, randomly select anyone.
VI. Construct non-dominated set of swarm, and this group is inserted in the achieve (A_t) based on the method in [42].
VII. Update the global best ($gbest_i$) for each particle in the swarm that are selected from the achieve (A_t).

Update the iteration number

End

Step-5

Until maximum number of iteration is reached.

End

5. RESULTS AND DISCUSSION

With an insertion of three-sided bar at adiabatic state in the pre-defined channel, firstly a numerical study has been executed on two-dimensional, laminar, steady state forced convection problem. The investigation has been conducted for diverse Reynolds number (Re=25, 50, 100, 200) and varied locations of vortex generator within the predefined channel in accordance to generate sufficient data to originate the prediction function. But the discussion is done only for fewer cases in this section. Using streamlines, the flow field structure is characterized. With uniform profile of temperature and uniform velocity, the fluid thrusts into the channel. The increment of Nusselt number due to bar insertion compared to the case of no bar is depicted in figure A3 (I). For all the cases, the Nusselt number of each block increases with the increase of Reynolds number.

The streamlines and temperature distribution are portrayed for Re=50 and 200 in figures A3(II) and A3(III) respectively for a fixed vortex position. The figures display nearly 1/3 fraction of the entire channel. Here the flow is diverted to the top of first block by the front face of the bar and also gets accelerated because of contraction between first block and edge of the bar. Specifically, in this particular part of the channel a jet-like demeanor is witnessed. A very small sized vortex is perceived at the back of the bar and also a weak circulation is formed between each blocks. The size as well as the number of vortex rearward the bar is increased with the enhancement of Reynolds number. Also an increase in strength of the fluid within the cavities between each blocks has been revealed with the raise of Reynolds number. Figure A3(II) explores the disparity of streamlines with the Reynolds number. Figure A3(II)(b) demonstrates that there are two circulation cells at the rear of the bar for Re=200. Adjacent the lower edge of the three-sided bar, comparatively large vortex is witnessed. The formation of a colossal recirculation rearward the fifth block and a second circulation between each blocks is depicted in the figure A3(II). The recirculation behind the fifth block is stretched out with the raise of Reynolds number. The outcomes depict the significant augmentation of heat transfer rate with the raise of Reynolds number.

For a changed Reynolds number whereas the bar inlaid at fixed spot (x=6b, y=4.5b) within the channel, isotherms are

pictured in figure A3(III). The fluid thrusts into the duct by an unvarying temperature as specified in the boundary conditions. A better thinning of thermal boundary layer for an increase of Reynolds number is witnessed. Figure A4 portrays the disparity of Nusselt number with apiece stricture of three-sided bar location and shape distinctly fixing some strictures each time. An overview of the numerical study through figure 4 delivers the information that bar position of y/b=5.5, and x/b=11 to 13 is lucrative in heat transmission augmentation whereas the base length disparity impacts not as much of comparatively, in view of individual blocks. Within the constrained strictures, relative to other blocks, the first block imitates healthier heat transmission. Making this function to minimal is the main objective.

Positioning the bar, a jiff away from blocks along y-axis provides superior thinning of thermal boundary layer, especially for first three blocks as witnessed in figure A5(a-c). The improvement in slimming of thermal boundary layer over second and third block is assimilated, moving the vortex creator along x-axis up to over second block. This occurrence evidently demonstrates that position of the vortex generator impacts a lot in augmentation process of heat transferal successfully. The diversion of air current by the hypotenuse of three-sided bar solely plays the key role in this event. The achievement of better Nusselt number over the blocks, at some specified bar positions depicted in figure. A4(a-b) is justified fruitfully. The improvement in uniformity of temperature distribution is perceived clearly in figure A5 for the bar position above the second block more willingly than other cases. Although heat augmentation process is perceived well for all the positions of vortex generator, at some specific locations, an enhanced uniformity of heat transmission is addressed. This fact comes up with the prominence of determining the optimal position of three-sided bar so as to attain the extreme as well as an even rate of heat transferal over the blocks. Figure A6 elucidates the disparity of the local Nusselt number on each surface of the blocks as shown in figure A1(a). The distance, and x axis of the figure implies the related surface of the block. Utilizing (3.11), the local Nusselt number is computed. Results are demonstrated for four altered cases depending upon the position of the bar along x axis, x/b=6, x/b=8, x/b=11, x/b=13. Highest local Nusselt number is found at top surface forefront of each block as the flow imposes to that point firstly. The upper faces B-C, F-G, J-K plays a significant role for heat transfer than the front and rare faces. Addition of a three-sided bar makes an improvement to eradicate heat from upper surface of each block especially for vortex creator position, x/b=13, which is shown in figure A6(a-c)). But this precise addition creates no optimistic exertion on rear faces C-D, G-L, K-L as depicted in figure A6(a-c). On this area, because of minor stream velocity, the current rate turns into squat. Fairly analogous situation is perceived for fore faces A-B, E-F and I-G. The finest augmentation of heat transmission is obtained at C-D as in figure A6(a) for the case x/b=13, which is a fascinating result to be addressed. Nonetheless, an enhanced heat transferal formation for vortex creator location y/h=4.5, x/h=13 turns as a consequence of the overall study.

5.1. Prediction of RSM

RSM is an empirical modeling approach for determining the relationship between various process parameters and responses with the various desired criteria and searching the significance of these process parameters on the coupled responses. In the current study, some functions defining the average Nusselt number of each blocks in different Reynolds number have been predicted by means of RSM in Minitab. For this purpose, for every functions, 96 input data in diverse positions of vortex creator (X=6b, 8b, 11b, 13b; Y=3.5h, 4.5h, 5.5h), which are the numerical solution of the governing equations, have been exerted. For the same Re=25, 50, 100, 200 and base, a/b=1, .0.5 is considered. To authenticate the outputs of the RSM model, some extra parameters of vortex creator positions are randomly considered (viz. x=7b, 9b, 10b, 12b at y=5.5b) and numerically calculated, and then a comparison between old and new CFD results and the prediction results are done. It is revealed that there is not much deviation in CFD and predicted results as in figure A7. According to figure A8, diverse positions of vortex creator in x-direction have been plotted, affixing randomly Reynolds number and vortex creator's vertical distance from bottom wall and its base length. For all

Reynolds numbers, the mean relative error of the Nusselt number of each block is given in table 2. According to table 2, all calculated errors are within acceptable range, and the predicted functions are reliable.

Table 2.Prediction function mean error % for the blocks

Re	Nu1	Nu2	Nu3	Nu5
25	0.656843	1.017373	0.385297	0.707919
50	0.355269	1.154296	2.657986	3.234201
100	0.043385	2.471288	1.284568	1.212535
200	0.044026	0.930684	0.736803	0.673581

The sensitivity of optimization of the current problem in accordance to reach maximum heat transfer rate is justified by depicting some contour plots for Re=87.23 as in figure A8. Considering each block individually, the position of vortex creator along x-axis, effects differently while for y-axis the effect remains almost the same. Vortex creator more closely to the blocks is advantageous individually.

5.2. Optimization results of PSO

Intel core i7 desktop with 8GB RAM is used for running the optimization model. In order to demonstrate the potentiality of MOPSO algorithm, simulation study is carried out using MATLAB. For the algorithms, the initial population chosen is 100. The parameters involved in MOPSO are as follows: the horizontal distance of vortex creator is from inlet, the vertical distance of vortex creator is from bottom wall and the Reynolds number. This heads to the generation of a set of Pareto front of Nu1 and Nu2 (Nu1 and Nu2 are average Nusselt Number of 1st and 2nd chip respectively. However, implementation of MOPSO consequences a number of non-dominated solutions for optimization of combination of responses viz. Nu1 and Nu2. The Pareto-optimal solutions obtained using through MOPSO are based on the ϵ dominance concept. Figure A9 depicts the Pareto-optimal solution for the present optimization model. It is clear that there are several optimal parameters, and among which six values are considered by combining the three sets viz. one set is for maximum 'Nu2' and minimum 'Nu1' (A & B), second set is for moderate 'Nu1' and 'Nu2' (C & D) and the third set is for 'Minimum 'Nu2' and maximum 'Nu1' (E & F). Table 3 summarizes the corresponding values of the input parameters with the required output of the six values. The optimization results fits more precisely with the numerical outputs. The two present objective functions are opposing in characteristics as concurrent improvement is impossible. It refers to the contrary attribute of the Pareto-optimal front, where when one function progresses, the other lowers or vice-versa.

Table 3.A set of input parameters with resultant objective function values

Point	X	Y	Re	Nu1	Nu2
A	12.92031	5.5	200	0.8712	0.5098
B	12.92031	5.5	200	0.8779	0.5097
C	12.77783	5.5	185.4126	0.9191	0.5036
D	12.77783	5.5	169.7096	0.9225	0.5031
E	12.58075	5.5	49.20805	0.9872	0.4955
F	12.43021	5.5	65.39892	0.9936	0.4951

6. CONCLUSIONS

This numerical study intends a hybrid, embedded technique of RSM blended with multi objective particle swarm optimization (MOPSO) for the optimization of the heat transfer process over electronic chips kept in a channel. The best solution is chosen from all the non-dominated solution using ϵ dominance concept. From the numerical observation and analysis, the following conclusion can be drawn.

- Insertion of the bar and its position's alteration especially along x-axis acts as a good passive technique in heat transferal augmentation over the blocks within the channel. This heat transfer increases with increase in Reynolds number.
- An increase in strength of the fluid within the cavities between each blocks has been revealed with the raise of Reynolds number.
- Comparatively a heat transfers uniformly over the first three blocks for the bar position (y/b=4.5 to 5.5; x/b=11 to 13) with uniform temperature distribution.
- Considering local Nusselt number, the position of bar at y=4.5b to 5.5b and x=11b to 13b influences better in heat transferal augmentation of front and upper faces for 1st three blocks. The front and upper faces of each block helps more in augmentation process compared to back faces.
- RSM is able to generate a prolific prediction function of Nusselt number with

a difference less than 3% for all Reynolds number with the actual numerical results.

- A set of Pareto optimal points is found out. The outcomes evidently reveal the level of conflict between two objective functions. The ultimate optimal point depends on the relative importance of the bar position and Reynolds number.
- The insertion of more number of vortex generator (VG) can be studied to demonstrate the heat transfer compared to the 1VG.
- The study may be extended in case of mixed convection to patterned heat transfer.

REFERENCES

[1] F.P.Incropera, Convection Heat Transfer in Electronic Equipment Cooling, Journal of Heat Transfer, Vol. 110, 1988, pp. 1097-1111, https://dx.doi.org/10.1115/1.3250613.

[2] A.E.Bergles, Recent Developments in Convective Heat Transfer Augmentation, Applied Mechanics Reviews, Vol. 26, No. 6, 1973, pp. 675-682.

[3] R.Sivasubramaniyam and K.Maniysundar, Performance Analysis and Heat Transfer Studies on Protruding Surfaces of Electronic Components, Concurrent Advances in Mechanical Engineering, Vol. 1, No. 1, 2015, pp. 37-60, http://dx.doi.org/10.18831/came/2015011005.

[4] R.L.Webb, Principles of Enhanced Heat Transfer, John Wiley Sons, UK, 1994.

[5] A.Ebrahimi, E.Roohi and S.Kheradmand, Numerical Study of Liquid Flow and Heat Transfer in Rectangular Microchannel with Longitudinal Vortex Generators, Applied Thermal Engineering, Vol. 78, 2015, pp. 576–583, https://dx.doi.org/10.1016/j.applthermaleng.2014.12.00.

[6] H.E.Ahmed, H.A.Mohammed and M.Z.Yusoff, An Overview on Heat Transfer Augmentation using Vortex Generators and Nanofluids: Approaches and Applications, Renewable and Sustainable Energy Reviews, Vol. 16, No. 8, 2012, pp. 5951–5993, https://dx.doi.org/10.1016/j.rser.2012.06.003.

[7] Avanish Singh Chahar and Vijay Kumar Dwivedi, Computational Investigation of Pressure Drift in Pipes of Shell and Tube Heat Exchanger, Concurrent Advances in Mechanical Engineering, Vol. 1, No. 1, 2015, pp. 1-8, http://dx.doi.org/10.18831/came/2015011001.

[8] Chunhua Min, Chengying Qi, Xiangfei Kong and Jiangfeng Dong, Experimental Study of Rectangular Channel with Modified Rectangular Longitudinal Vortex Generators, International Journal of Heat and Mass Transfer, Vol. 53, No. 15–16, 2010, pp. 3023–3029, https://dx.doi.org/10.1016/j.ijheatmasstransfer.2010.03.026.

[9] Charbel Habchi, Serge Russeil, Daniel Bougeard, Jean-Luc Harion, Thierry Lemenand, Dominique Della Valle and Hassan Peerhossaini, Enhancing Heat Transfer in Vortex Generator-Type Multifunctional Heat Exchangers, Applied Thermal Engineering, Vol. 38, 2012, pp. 14–25, https://dx.doi.org/10.1016/j.applthermaleng.2012.01.020.

[10] A.Sh.Kherbeet, H.A.Mohammed, Hamdi E.Ahmed, B.H.Salman, Omer A.Alawi, Mohammad Reza Safaei and M.T.Khazaal, Mixed Convection Nanofluid Flow over Microscale Forwardfacing Step — Effect of Inclination and Step Heights, International Communications in Heat and Mass Transfer, Vol. 78, 2016, pp. 145–154, https://dx.doi.org/10.1016/j.icheatmasstransfer.2016.08.016.

[11] A.Sh.Kherbeet, Mohammad Reza Safaei, H.A.Mohammed, B.H.Salman, Hamdi E.Ahmed, Omer A.Alawi and M.T.Al-Asadi, Heat Transfer and Fluid Flow Over Microscale Backward and Forward Facing Step: a Review, International Communications in Heat and Mass Transfer, Vol. 76, 2016, pp. 237–244, https://dx.doi.org/10.1016/j.icheatmasstransfer.2016.05.022.

[12] Kai-Shing Yang, Jhih-Hao Jhong, Yur-Tsai Lin, Kuo-Hsiang Chien and Chi-Chuan Wang, On the Heat Transfer Characteristics of Heat Sinks: with and without Vortex Generators, IEEE Transactions on Components and Packaging Technologies, Vol. 33, No. 2, 2010, pp. 391–397, https://dx.doi.org/10.1109/TCAPT.2010.2044412.

[13] Chen Chen, Jyh-TongTeng, Ching-Hung Cheng, Shiping Jin, Suyi Huang, Chao Liu, Ming-Tsang Lee, Hsin-Hung Pan and Ralph Greif, A Study on Fluid Flow and Heat Transfer in Rectangular Microchannel with various Longitudinal Vortex Generators, International Journal of Heat and Mass Transfer, Vol. 69, 2014, pp. 203–214, https://dx.doi.org/10.1016/j.ijheatmasstransfer.2013.10.018.

[14] Chao Liu, Jyh-tong Teng, Jian-Cherng Chu, Yi-lang Chiu, Suyi Huang, Shiping Jin, Thanhtrung Dang, Ralph Greif and Hsin-Hung Pan, Experimental Investigations on Liquid Flow and Heat Transfer in Rectangular Microchannel with Longitudinal Vortex Generators, International Journal of Heat and Mass Transfer, Vol. 54, No. 13–14, 2011, pp. 3069–3080, https://dx.doi.org/10.1016/j.ijheatmasstransfer.2011.02.030.

[15] H.Mirzaee, Abdolrahman Dadvand, I.Mirzaee and R.Shabani, Heat Transfer Enhancement in Microchannels using an Elastic Vortex Generator, Vol. 19, No. 3, 2012, pp. 199–211, https://dx.doi.org/10.1615/JEnhHeatTransf.2012002747 .

[16] A.Sohankar and L.Davidson, Effect of Inclined Vortex Generators on Heat Transfer Enhancement in a Three-Dimensional Channel, Numumerical Heat Transfer Part A, Vol. 39, 2001, pp. 433–448.

[17] S.J.Yang, A Numerical Investigation of Heat Transfer Enhancement for Electronic Devices Using an Oscillating Vortex Generator, Numerical Heat Transfer Part A, Vol. 42, 2002, pp. 269–284, https://dx.doi.org/10.1080/10407780290059549.

[18] H.W.Wu and S.W.Perng, Effect of an Oblique Plate on the Heat Transfer Enhancement of Mixed Convection Over Heated Blocks in a Horizontal Channel, International Journal of Heat Mass Transfer, Vol. 42, No. 7, 1999, pp. 1217–1235, https://dx.doi.org/10.1016/S0017-9310(98)00247-6.

[19] A.Valencia, Heat Transfer Enhancement Due to Self-Sustained Oscillating Transverse Vortices in Channels with Periodically Mounted Rectangular Bars, International Journal of Heat Mass Transfer, Vol. 42, No. 11, 1999, pp. 2053–2062, https://dx.doi.org/10.1016/S0017-9310(98)00295-6.

[20] S.Alahyari Beig, E.Mirzakhalili and F.Kowsari, Investigation of Optimal Position of a Vortex Generator in a Blocked Channel for Heat Transfer Enhancement of Electronic Chips, International Journal of Heat and Mass Transfer, Vol. 54, No. 19-20, 2011, pp. 4317–4324, https://dx.doi.org/10.1016/j.ijheatmasstransfer.2011.05.013.

[21] G.E.P.Box and K.B.Wilson, On the Experimental Attainment of Optimum Conditions, Journal of the Royal Statistical Society, Vol. 13, No. 1, 1951, pp. 1-45.

[22] J.Zhou, M.Hatami, D.Song and D.Jing, Design of Microchannel Heat Sink with Wavy Channel and its Time-Efficient Optimization with Combined RSM and FVM Methods, International Journal of Heat And Mass Transfer, Vol. 103, 2016, pp. 715-724, https://dx.doi.org/10.1016/j.ijheatmasstransfer.2016.07.100.

[23] Huai-Zhi Han, Bing-Xi Li, Hao Wu, and Wei Shao, Multi-Objective Shape Optimization of Double Pipe Heat Exchanger with Inner Corrugated Tube Using RSM Method, International Journal of Thermal Sciences,Vol. 90, 2015, pp. 173-186, https://dx.doi.org/10.1016/j.ijthermalsci.2014.12.010.

[24] Sina Lohrasbi, Mohsen Sheikholeslami and Davood Domiri Ganji, Multi-

Objective RSM Optimization of Fin Assisted Latent Heat Thermal Energy Storage System Based on Solidification Process of Phase Change Material in Presence of Copper Nanoparticles, Applied Thermal Engineering, Vol. 118, 2017, pp. 430–447, https://dx.doi.org/10.1016/j.applthermaleng.2017.03.005.

[25] J.Grum and J.M.Slabe, The use of Factorial Design and Response Surface Methodology for Fast Determination of Optimal Heat Treatment Conditions of Different Niecoemo Surfaced Layers, Jounal of Materials Processing Technology, Vol. 155, 2004 pp. 2026-2032, https://dx.doi.org/10.1016/j.jmatprotec.2004.04.220.

[26] Babur Ozcelik and Tuncay Erzurumlu, Determination of Effecting Dimensional Parameters on Warpage of Thin Shell Plastic Parts using Integrated Response Surface Method and Genetic Algorithm, International Communication Heat and Mass Transfer, Vol. 32, No. 8, 2005, pp. 1085-1094, https://dx.doi.org/10.1016/j.icheatmasstransfer.2004.10.032.

[27] H.Oktem, T.Erzurumlu and H.Kurtaran, Application of Response Surface Methodology in the Optimization of Cutting Conditions for Surface Roughness, Journal of Materials Processing Technology, Vol. 170, No. 1-2, 2005, pp. 11-16, https://dx.doi.org/10.1016/j.jmatprotec.2005.04.096.

[28] S.K.Mandal, Dipak Sen and Asis Giri, Multi Objective Optimization of Laminar Mixed Convective Heat Transfer of Electronic Chips in a Horizontal Channel with Vortex Generator, International Journal of Mechanical and Production Engineering Research and Development, Vol. 8, No. 1, 2018, pp. 155-166.

[29] D.Calcada, A.Rosa, L.C.Duarte and V.V.Lopes, Comparison of GA and PSO Performance in Parameter Estimation of Microbial Growth Models: a Case-study Using Experimental Data, IEEE Congress on Evolutionary Computation, Spain, 2010, pp. 1–8, https://dx.doi.org/10.1109/CEC.2010.5586489.

[30] J.Kennedy and R.C.Eberhart, Particle Swarm Optimization, IEEE International Conference on Neural Networks, Australia, Vol. 1948, 1995, pp. 1942–1948.

[31] R.V.Rao and V.K.Patel, Thermodynamic Optimization of Cross Flow Plate-Fin Heat Exchanger Using a Particle Swarm Optimization Algorithm, International Journal of Thermal Sciences, Vol. 49, No. 9, 2010, pp. 1712–1721, https://dx.doi.org/10.1016/j.ijthermalsci.2010.04.001.

[32] Hao Peng, Xiang Ling and En Wu, An Improved Particle Swarm Algorithm for Optimal Design of Plate-Fin Heat Exchangers, Industrial and Engineering Chemistry Research, Vol. 49, No. 13, 2010, pp. 6144–6149. https://dx.doi.org/10.1021/ie1002685.

[33] M.Yousefi and A.Darus, Optimal Design Of Plate-Fin Heat Exchangers By Particle Swarm Optimization, International Conference on Machine Vision: Computer Vision and Image Analysis; Pattern Recognition and Basic Technologies, Singapore, Vol. 8350, 2011, https://dx.doi.org/10.1117/12.920912.

[34] H.Azarkish, S.Farahat and S.M.H.Sarvari, Comparing the Performance of the Particle Swarm Optimization and the Genetic Algorithm on the Geometry Design of Longitudinal Fin, International Journal of World Science and Engineering Investigation, Vol. 1, No. 1, 2012, PP. 70–74.

[35] Prasenjit Dey and Ajoy Kumar Das, A Utilization of GEP (Gene Expression Programming) Metamodel and PSO (Particle Swarm Optimization) Tool to Predict and Optimize the Forced Convection Around a Cylinder, Energy, Vol. 95, 2016, PP. 447-458. https://dx.doi.org/10.1016/j.energy.2015.12.021.

[36] Hakan F.Oztop, Yasin Varol and Dogan E.Alnak, Control of Heat

Transfer and Fluid Flow Using a Triangular Bar in Heated Blocks Located in a Channel, International Communication Heat and Mass Transfer, Vol. 36, No. 8, 2009, pp. 878–885, https://dx.doi.org/10.1016/j.icheatmasstransfer.2009.05.006.

[37] R.Eberhart and J.Kennedy, A New Optimizer using Particle Swarm Theory, International Symposium on Micro Machine and Human Science, Japan, 1995, pp. 39–43, https://dx.doi.org/10.1109/MHS.1995.494215.

[38] J.Kennedy and R.Eberhart, Particle Swarm Optimization, IEEE International Conference on Neural Networks, Australia, 1995, pp. 1942–1948.

[39] Ioan Cristian Trelea, The Particle Swarm Optimization Algorithm: Convergence Analysis and Parameter Selection, Information Processing Letters, Vol. 85, No. 6, 2003, pp. 317–325, https://dx.doi.org/10.1016/S0020-0190(02)00447-7.

[40] Xiaoyong Liu, Radial Basis Function Neural Network Based on PSO with Mutation operation to Solve Function Approximation Problem, International Conference In Swarm Intelligence, Berlin, 2010, pp. 92–99.

[41] R.Eberhart and J.Kennedy, A New Optimizer Using Particle Swarm Theory, IEEE International Symposium on Micro Machine and Human Science, Japan, 1995, pp. 39–43, https://dx.doi.org/10.1109/MHS.1995.494215.

[42] Ajay Singh and Bireswar Paul, Numerical Study of Convection Heat Transfer using Nano-fluid in the Developing Region of a Tube Flow, Journal of Advances in Mechanical Engineering and Science, Vol. 1, No. 3, 2015, pp. 14-20, http://dx.doi.org/10.18831/james.in/201503100 2.

[43] Y.Shi, Particle Swarm Optimization: Developments, Applications and Resources, IEEE Congress on Evolutionary Computation, Douth Korea, Vol. 1, 2001, pp. 81–86, https://dx.doi.org/10.1109/CEC.2001.934374.

[44] R.Marinke, E.Araujo, L.S.Coelho and I.Matiko, Particle Swarm Optimization (PSO) Applied to Fuzzy Modeling in a Thermal-Vacuum System, IEEE International Conference on Hybrid Intelligent Systems, Brazil, 2005, pp. 6, https://dx.doi.org/10.1109/ICHIS.2005.85.

[45] Jovita Nenortaite and Rimantas Butleris, Application of Particle Swarm Optimization Algorithm to Decision Making Model Incorporating Cluster Analysis, IEEE Conference on Human System Interactions, Poland, 2008, pp. 88–93, https://dx.doi.org/10.1109/HSI.2008.4581414.

[46] T.Aseer Brabin and S.Ananth, Analysis of Overall Heat Transfer Coefficient and Effectiveness in Split Flow Heat Exchanger using Nano Fluids, Journal of Advances in Mechanical Engineering and Science, Vol. 1, No.3, 2015, pp. 28-40, http://dx.doi.org/10.18831/james.in/201503100 4.

[47] S.V.Patankar, Numerical Heat Transfer and Fluid Flow, Hemisphere, New York, 1980.

[48] Jiang Hao and Zheng Jin-hua, Multi-Objective Particle Swarm Optimization Algorithm Based on Enhanced E-Dominance, IEEE International Conference on Engineering of Intelligent Systems, Pakistan, 2006, pp. 1-5, https://dx.doi.org/10.1109/ICEIS.2006.1703200.

APPENDIX A

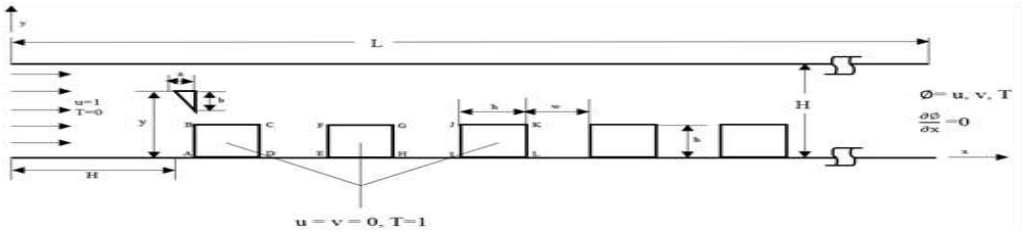

(a)

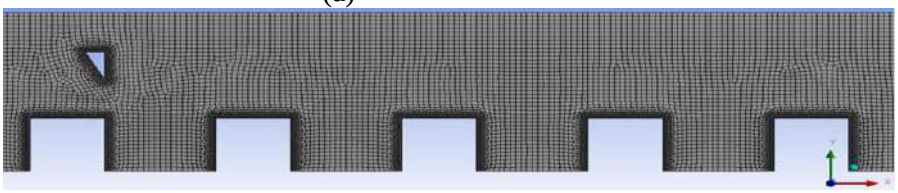

(b)

Figure A1.Schematic representation of physical model with dimensions and coordinates (a) Model with points to define calculation of local Nusselt number, (b) Grid distribution

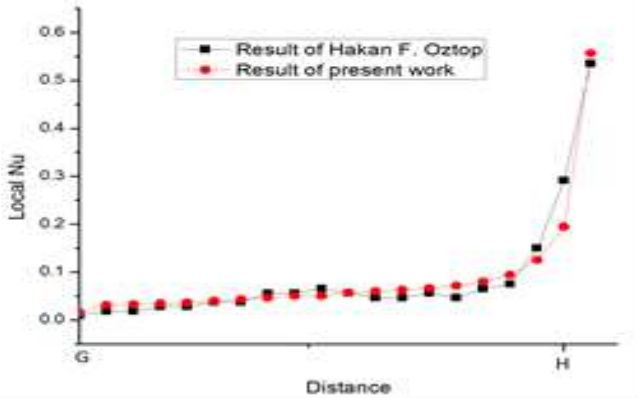

(a)

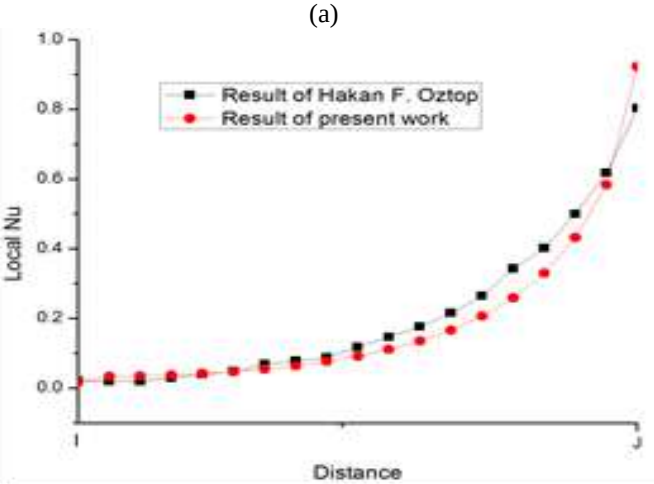

(b)

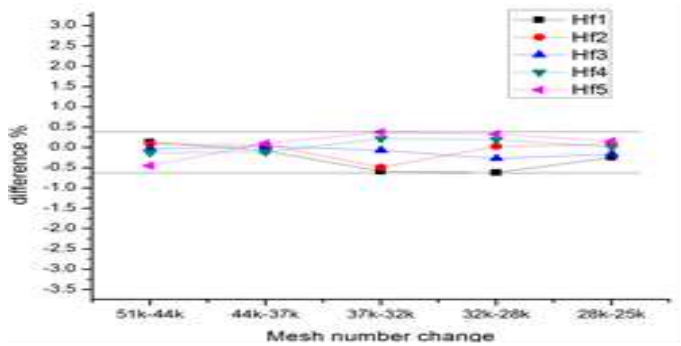

(c)

Figure A2.Validation of results of Local Nusselt number distribution of present work with Hakan F. Oztop [36], (a) 2nd block back face (b) 3rd block front face for Re=400,x/b=6,y/b=3.5 (c) Grid independency test of Nusselt number of each block for vortex position x/b=8,y/b=4.5 and Re=25, for present work

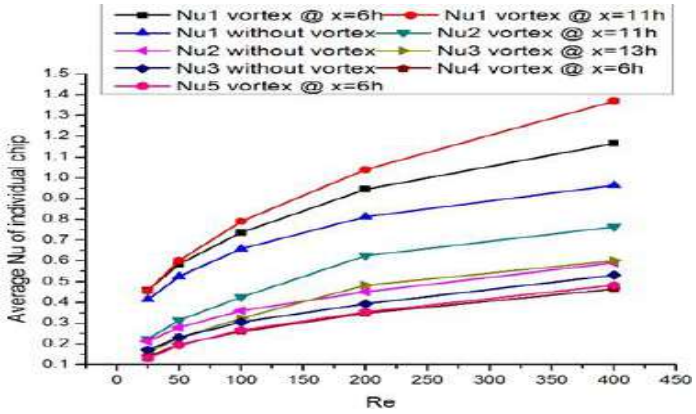

(I)

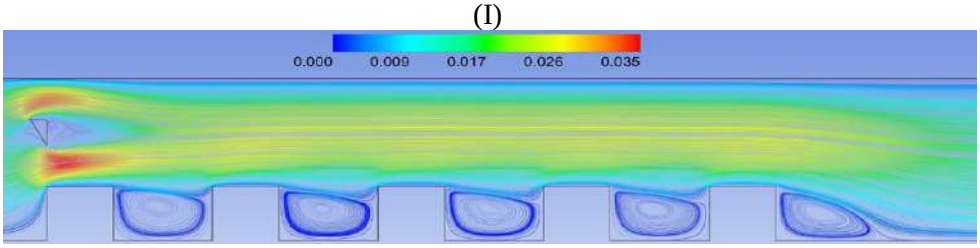

II(a)

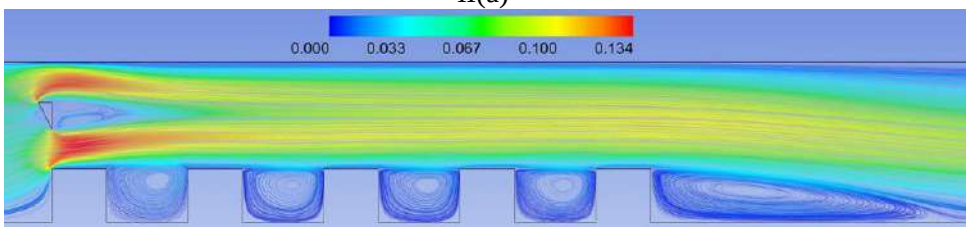

II(b)

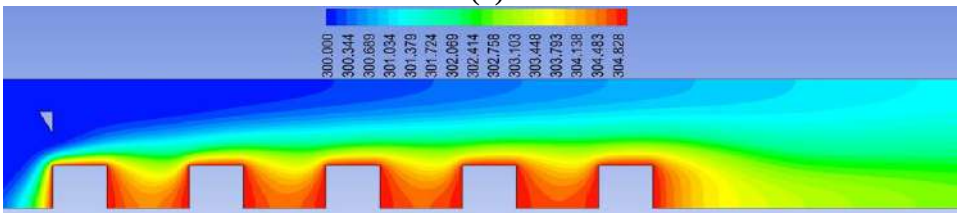

III(a)

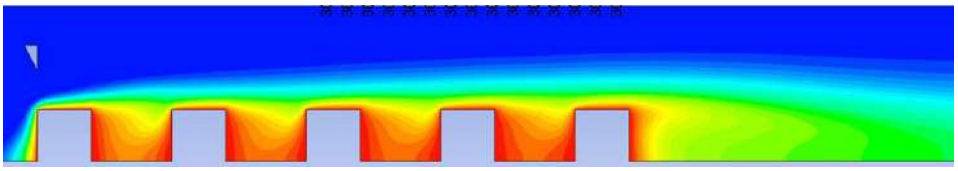

III(b)

FigureA3.(I) Disparity of Nusselt number of each block with Re at different positions of bar, (II) Velocity streamlines in m/s at X=6h, Y=4.5h, B=0.5h and Reynolds number, (a) Re=50, (b) Re=200, (III) Isotherms at X=6h,Y=4.5H, B=0.5h, and Reynolds number (a) Re=50, (b) Re=200

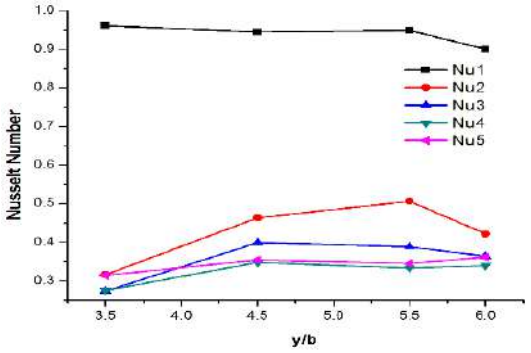

4(a)

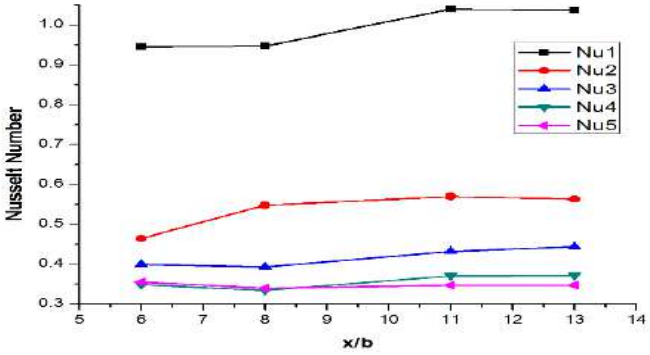

4(b)

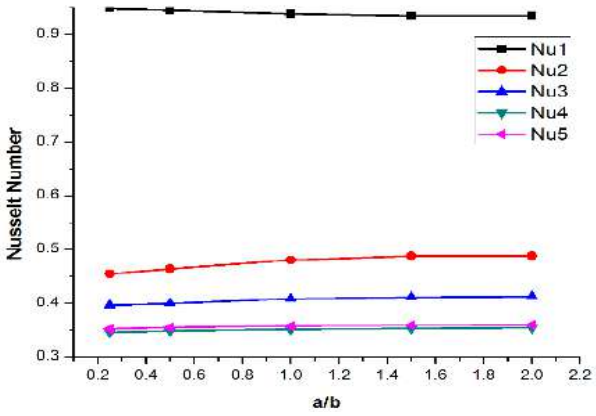

4(c)

Figure A4.Disparity of Nusselt number with some strictures fixing Re=200, (a) bar position along y-axis at x/b=6, (b) bar position along x-axis at y/b=4.5, (c) base length of bar

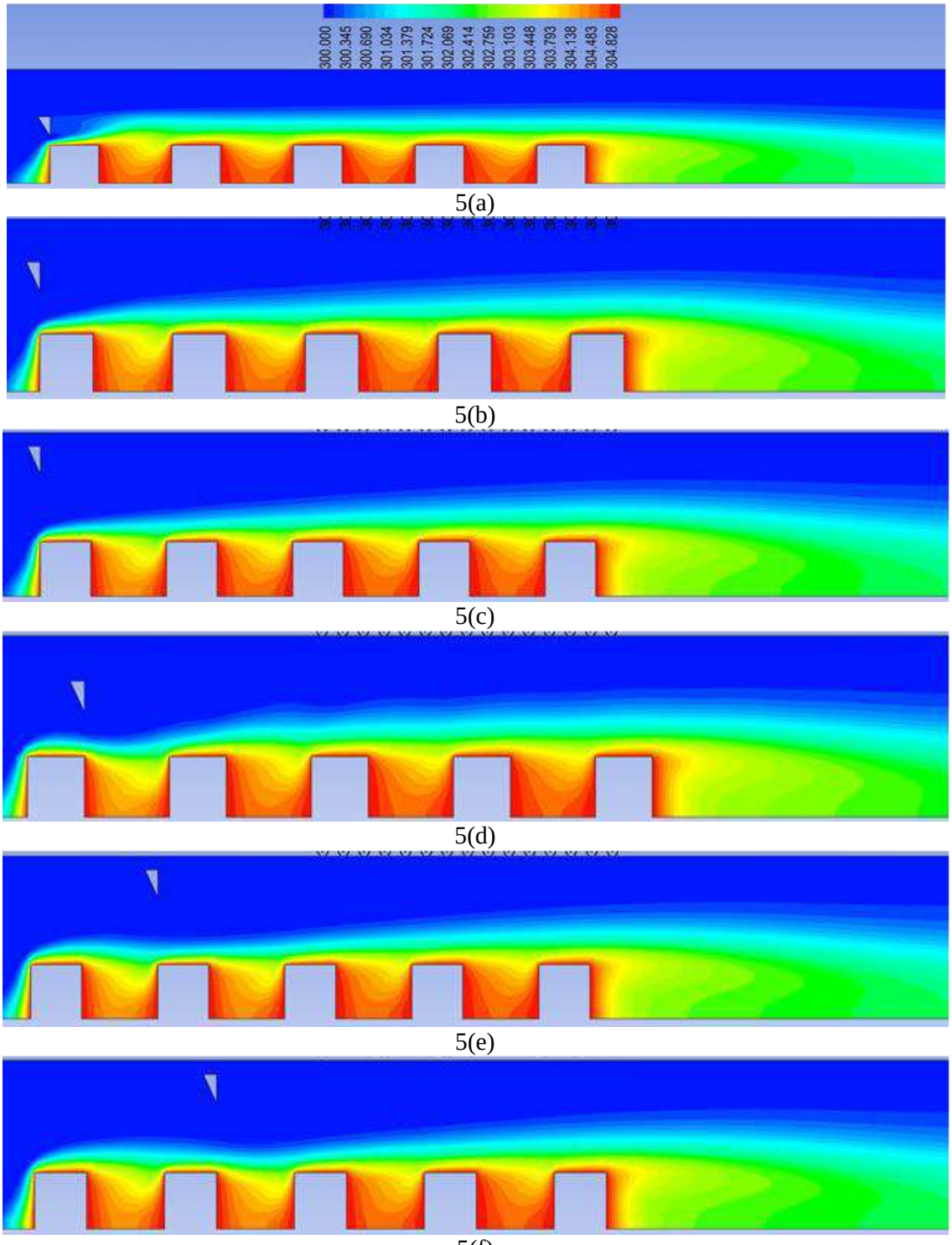

5(a)

5(b)

5(c)

5(d)

5(e)

5(f)

Figure A5.Deviation of temperature contours with alteration of bar location fixing Re=200 (a) x/b=6, y/b=3.5, (b) x/b=6, y/b=4.5, (c) x/b=6, y/b=5.5, (d) x/b=8, y/b=4.5, (a) x/b=11, y/b=5.5, (a) x/b=13, y/b=5.5

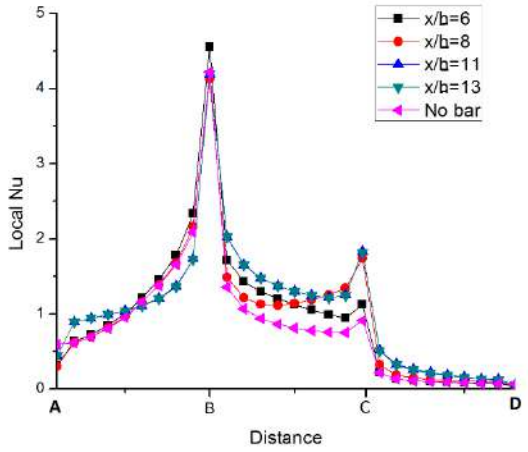

6(a)

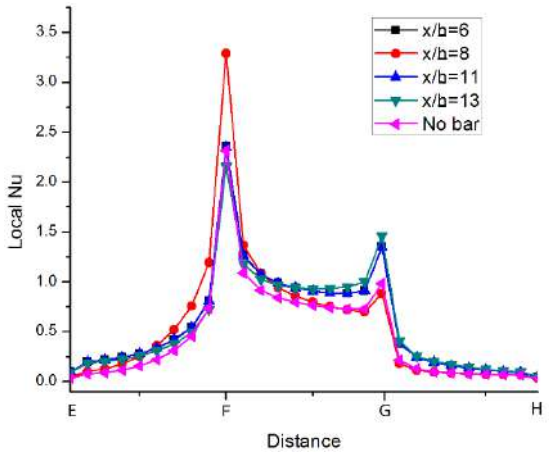

6(b)

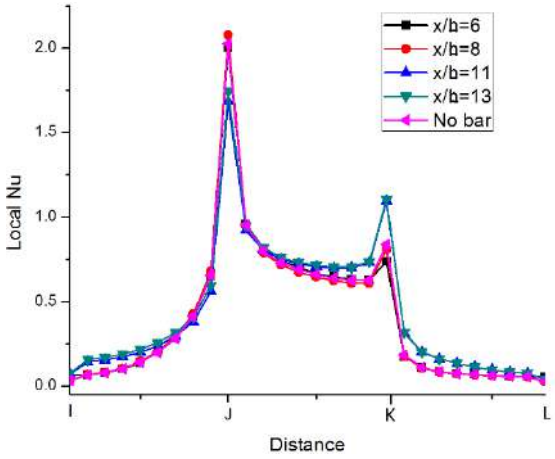

6(c)

Figure A6.Local Nusselt number disparity over the whole block surface at different bar positions along x-axis (a) block 1 (b) block 2 (c) block 3, for y/b=4.5, Re=200, a/b=.5

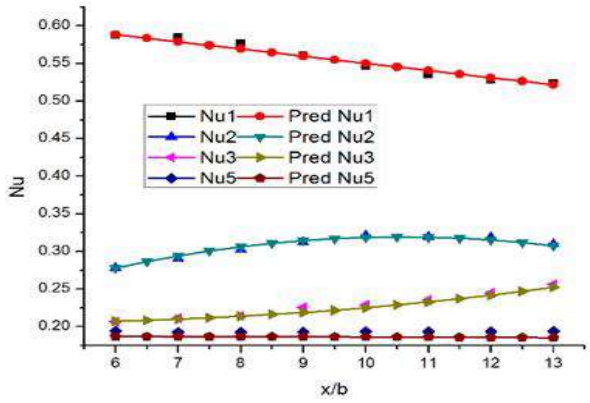

Figure A7.Comparison between predicted function and CFD results for Nusselt number of the blocks at bar position y=5.5b; a=b, Re=50

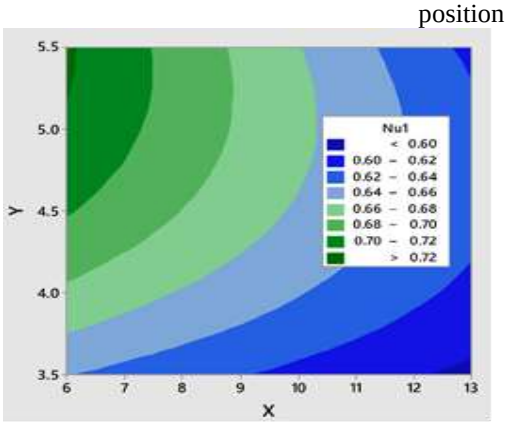

8(a)

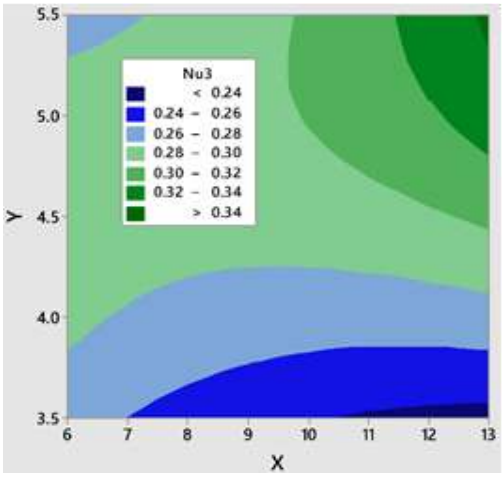

8(c)

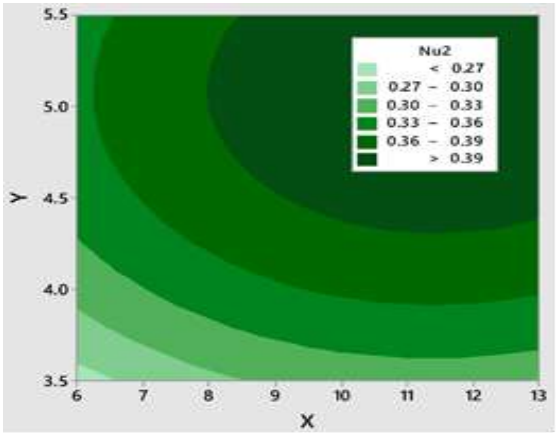

8(b)

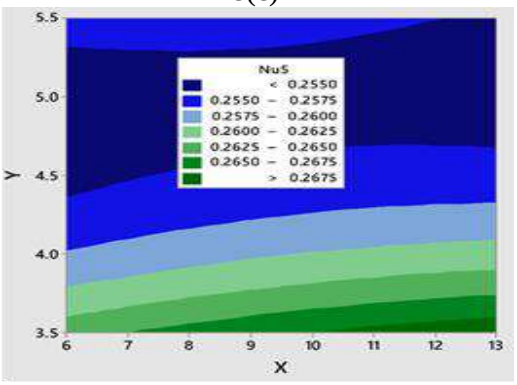

8(d)

Figure A8.Contour plots of Nusselt number for (a) Nu1 (b) Nu2 (c) Nu3 (d) Nu5 with holding value of Re=87.23

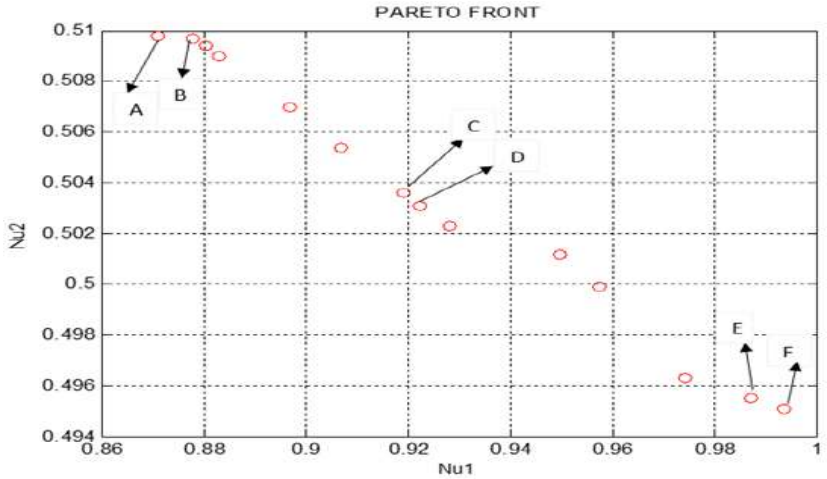

Figure A9.Pareto front for objectives: Nu1 and Nu2